Ultrabroadband continuum amplification in the near infrared using BiB_3O_6 nonlinear crystals pumped at 800 nm

Ivaylo Nikolov,[1] Alexander Gaydardzhiev,[1] Ivan Buchvarov,[1,*] Pancho Tzankov,[2] Frank Noack,[2] and Valentin Petrov[2]

[1]*Department of Physics, Sofia University, 5 James Bourchier Boulevard, BG-1164 Sofia, Bulgaria*
[2]*Max-Born-Institute for Nonlinear Optics and Ultrafast Spectroscopy, 2A Max-Born-Strasse, D-12489 Berlin, Germany*
**Corresponding author: ibuch@phys.uni-sofia.bg*

Received August 21, 2007; revised October 16, 2007; accepted October 19, 2007; posted October 25, 2007 (Doc. ID 86753); published November 13, 2007

Ultrabroadband parametric amplification of a white-light continuum in the near IR (~100 THz, 1.2–2.4 μm) is demonstrated in BiB_3O_6 pumped by 45 fs long pulses at 800 nm at a repetition rate of 1 kHz. The energy obtained with a 5 mm thick crystal reached 50 μJ, corresponding to external conversion efficiency of 20%. © 2007 Optical Society of America

OCIS codes: 190.4970, 320.7110.

During the past few years the generation of ultrabroadband coherent optical radiation had a substantial impact on numerous applications: some examples include time-resolved broadband pump–probe spectroscopy [1], optical tomography [2], near-field spectroscopy of nanoparticles [3], and generation of single-cycle optical pulses [4]. The commonly used technique to obtain ultrabroadband (more than one octave) coherent radiation is based on white-light generation in transparent materials using femtosecond lasers [5]. However, the achievable pulse energies of single-filament white-light continuum (WLC) sources at 1 kHz repetition rate are still very low (typically tens of nanojoules), which limits their applicability. The concept of ultrabroadband coherent amplification (or generation when starting from the parametric superfluorescence) relies on optical parametric amplification (OPA) at an achromatic phase-matching condition defined by zero group velocity mismatch (GVM) between idler and signal pulses along the direction of the signal wave vector [6]. In the case of collinear type I interaction, this condition is always fulfilled near degeneracy ($\lambda_S \approx \lambda_I$), but the bandwidth can be further enhanced if the group velocity dispersion (GVD) of the signal and idler waves also vanishes [7,8]. For a number of birefringent nonlinear crystals, this ultrabroad gain bandwidth occurs at some specific pump wavelength [8], not necessarily within the spectral range of operation of technologically established lasers. For instance, in BBO this situation is realized for a pump wavelength λ_P around 665 nm [8], far from the 800 nm spectral range in which high-power femtosecond Ti:sapphire based laser systems operate with high stability at kilohertz repetition rates. As shown recently, similar conditions can also be realized in periodically poled materials such as periodically poled $KTiOPO_4$ (KTP) where the optimum pump wavelength is about 900 nm [9].

In this Letter we report on ultrabroadband OPA in the relatively new nonlinear crystal bismuth triborate, BiB_3O_6 (BIBO), pumped by a 1 kHz Ti:sapphire laser amplifier (λ_P=800 nm). The proposed type of interaction ($e \rightarrow oo$) in the x–z principal plane brings together ultrabroad amplification bandwidth, high effective nonlinearity [$d_{eff}(\mathrm{BIBO}) = d_{12} \cos\theta$ = 3.14 pm/V at λ_S=1400 nm; higher than d_{eff}(KTP)], and small GVM between the amplified and pump pulses.

The parametric gain bandwidth can be qualitatively analyzed in the plane-wave approximation assuming that the pump is monochromatic and remains undepleted. Direct calculation using the recently refined Sellmeier coefficients of BIBO [10] predicts an ultrabroad amplification band, extending roughly from 1.2 to 2.4 μm, as shown Fig. 1(a).

The origin of this ultrabroad amplification bandwidth is easy to explain using simple analytical expressions derived under the same approximations. The gain bandwidth at a certain signal frequency ω_S is defined by the frequency values for which the gain drops to 50% of its maximum value, which occurs for a wave vector mismatch Δk ($\Delta k = k_P - k_S - k_I$) determined from the equation $\Delta k(\omega_S, \omega_I) = \sqrt{(4\Gamma \ln 2/L)}$, where k_P, k_S, and k_I are the wave vectors of the pump, signal, and idler waves, respectively, ω_S and ω_I are the signal and the corresponding idler frequency, respectively; Γ is the exponential parametric gain coefficient [6,11]; and L is the crystal length. To obtain analytical expressions for the parametric gain bandwidth the wave vector mismatch $\Delta k(\omega_S, \omega_I)$ can be expanded as a Taylor series with respect to the frequency around the phase-matching point $\Delta k(\omega_S, \omega_I) = 0$. If the signal frequency change is $\Delta\omega_S = \Delta\omega$, by energy conservation the idler frequency change will be $\Delta\omega_I = -\Delta\omega$. Therefore, at a given crystal length and pump intensity I_P, the amplification bandwidth $\Delta\omega$ is inversely proportional to the first nonzero coefficient of the Taylor expansion, in the order starting with the GVM between signal and idler, the sum of the GVD of the signal and the idler waves, and so on. Fig-

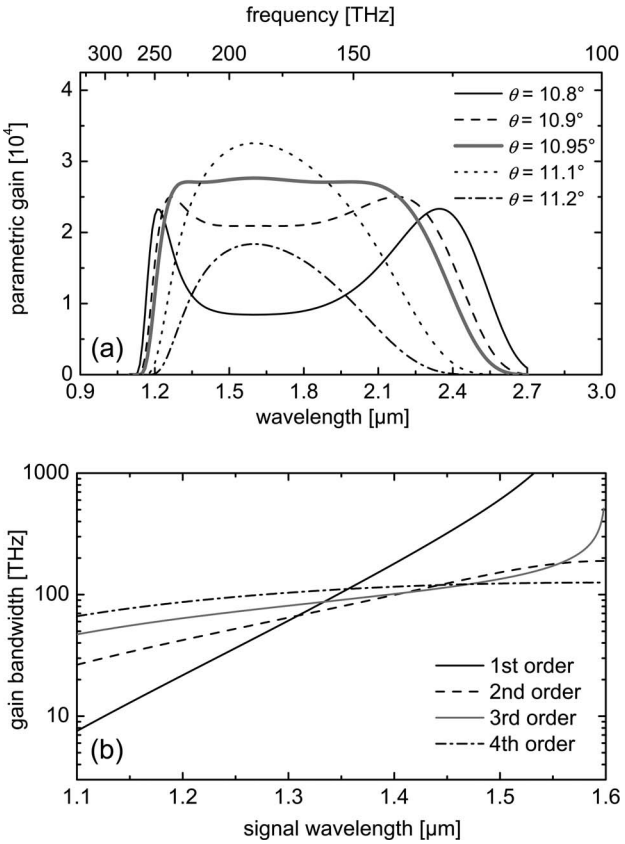

Fig. 1. (a) Parametric gain of BIBO for collinear type $e \rightarrow oo$ interaction at $\lambda_P = 800$ nm calculated for several fixed phase-matching angles close to degeneracy ($\theta = 11.05°$). The crystal length (3 mm) and the pump intensity (60 GW/cm^2) correspond to the experimental conditions. (b) Gain bandwidth (FWHM) of BIBO, analytically calculated for the same parameters as in (a) using only the first-, second-, third-, and fourth-order Taylor series expansion terms of the wave vector mismatch Δk, respectively.

ure 1(b) shows the contribution of the individual terms of the Taylor expansion of the wave vector mismatch $\Delta k(\omega_S, \omega_I)$ at the phase-matching point, calculated using such analytical formulas. At degeneracy, $\omega_S = \omega_I$, all odd coefficients of the Taylor expansion become zero. In BIBO pumped at 800 nm, by chance at $\lambda_S = 1580$ nm, which almost coincides with the degeneracy point, the signal and idler GVD also vanish. Therefore, the parametric amplification possesses ultrabroad bandwidth, which can be approximately calculated using the fourth-order coefficient of the Taylor expansion, from

$$\Delta\nu_{FWHM} = \Delta\omega_{FWHM}/2\pi = \frac{2(9\ln 2)^{1/8}}{\pi}\left(\frac{\Gamma}{L}\right)^{1/8}\left|\frac{\partial^4 k_S}{\partial\omega_S^4} + \frac{\partial^4 k_I}{\partial\omega_I^4}\right|^{-1/4},$$

with a result very similar to the direct calculation in Fig. 1(a).

On the other hand the efficiency of OPA is limited for ultrashort laser pulses by the GVM between the pump and amplified (signal, idler) pulses. In the case of $e \rightarrow oo$ interaction in BIBO there is quite a broad spectral range near $\lambda_S = 1300$ nm where the signal and idler pulses travel with group velocities very close to that of the pump. This interesting property is related to the fact that the pump wavelength ($\lambda_P = 800$ nm) is close to the point where the second harmonic (818.5 nm) has the same group velocity as the fundamental (1637 nm).

These exceptional properties of BIBO are demonstrated by WLC amplification in the much simpler for realization collinear geometry (Fig. 2). Since continua generated from 800 nm exhibit strongly decreasing intensity towards 1600 nm, we used as a seed the anti-Stokes part of the WLC generated in a 3 mm thick YAG by 50 fs pulses at 2.1 μm. YAG was chosen because from several fluoride and oxide materials tested, it provided the most stable WLC without any sign of damage. The uncoated 3 and 5 mm thick BIBO crystals were cut at $\theta = 11.4°$. The average pump intensity (half of the peak on-axis level) at 800 nm was 60 GW/cm^2.

Typical maximum energies of the amplified WLC were 30 and 50 μJ for the 3 and 5 mm thick BIBO crystals, respectively. These values were obtained for pump delays that simultaneously provided ultrabroad bandwidths of the amplified WLC. Thus the maximum intrinsic conversion efficiency was 20% for the 5 mm thick BIBO. The amplified WLC spectrum in the case of 3 mm thick BIBO is shown in Fig. 3(a). The partial spectrum up to 1600 nm (thick solid curve) was directly recorded by an InGaAs-based spectrometer, while the complete spectrum shown by dashed curve was reconstructed from the cross-correlation frequency-resolved optical gating (XFROG) trace, which was recorded with a VIS spectrometer; see Fig. 4. Finally, the thick gray curve in Fig. 3(a) shows the portion of the amplified spectrum (>1600 nm) that was calculated from the one directly measured below 1600 nm, using the Manley–Rowe relation. Analogous curves are presented in Fig. 3(b) for the 5 mm thick BIBO. The obtained amplification bandwidth was ~80 THz for the 3 mm thick BIBO, and it increased to ~100 THz in the case of the 5 mm thick BIBO. The FWHM of the cross-correlation functions recovered from the XFROG measurement were 84 fs [see the inset of Fig. 3(a)] and 105 fs for the 3 and 5 mm thick BIBO crystals, respectively, i.e., the corresponding amplified WLC pulse durations are

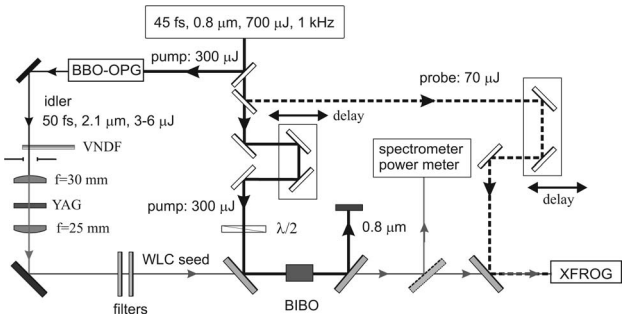

Fig. 2. Experimental setup: VNDF, variable neutral density filter; filters, Ho:YAG mirrors reflecting the 2.1 μm pump; XFROG, cross-correlation frequency-resolved optical gating based on sum-frequency generation in a 10 μm thick, type I ($oo \rightarrow e$) BBO crystal.

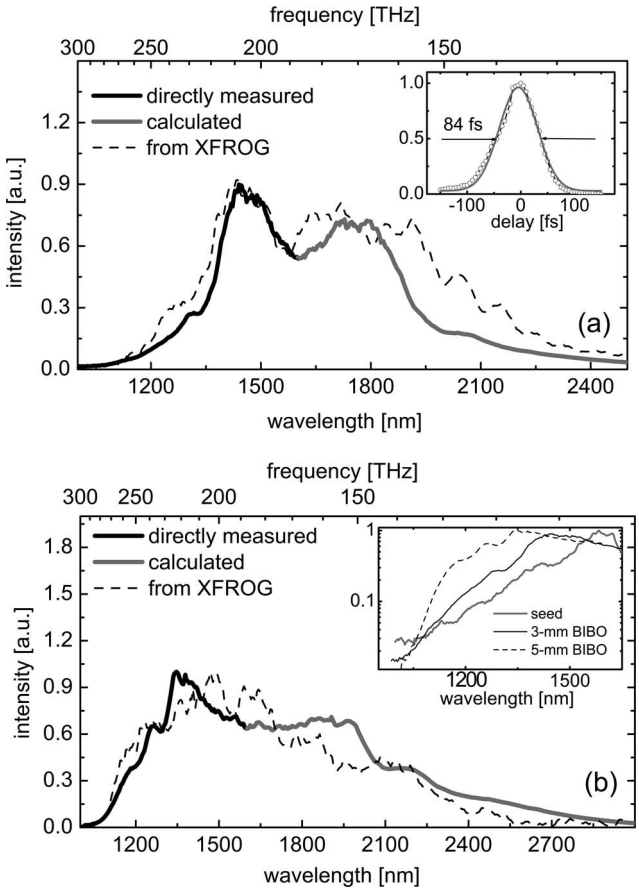

Fig. 3. Spectra of the WLC amplified in (a) 3 mm and (b) 5 mm thick BIBO, measured by the InGaAs spectrometer (thick solid curve), reconstructed from the time-integrated XFROG trace (dashed curve), and computed from the Manley–Rowe relation (gray curve). The inset in (a) shows a cross-correlation function with a Gaussian fit of the amplified WLC in the 3 mm BIBO; the inset in (b) is a comparison of the spectra of the WLC seed generated in YAG (gray curve) and the amplified WLC in the 3 mm (solid curve) and 5 mm (dashed curve) thick BIBO crystals.

~70 and ~95 fs, 1.4 and 1.9 times longer than the pump pulses at 2.1 μm, respectively.

The simultaneous increase of the spectral width and pulse duration for the longer BIBO crystal can only be explained by involving chirp effects. In that case the increasing temporal walk-off between the pump and amplified pulse results in spectral broadening. The WLC seed level did not allow the direct characterization of its temporal and spectral properties. However, from estimations of the GVD in all optical elements used (including the YAG and BIBO crystals) we conclude that the main source of chirp is the BIBO crystal itself. This is not unexpected since this material exhibits the lowest bandgap. Since the zero GVD point is near the 1600 nm degeneracy point, the chirp produced by GVD in BIBO has the opposite sign for the signal and idler frequencies, which can be seen in Fig. 4. While this satisfies the requirement for energy conservation in the case of OPA pumped by monochromatic pump, it is clear that compensation of such chirp in subsequent pulse compression schemes is not trivial.

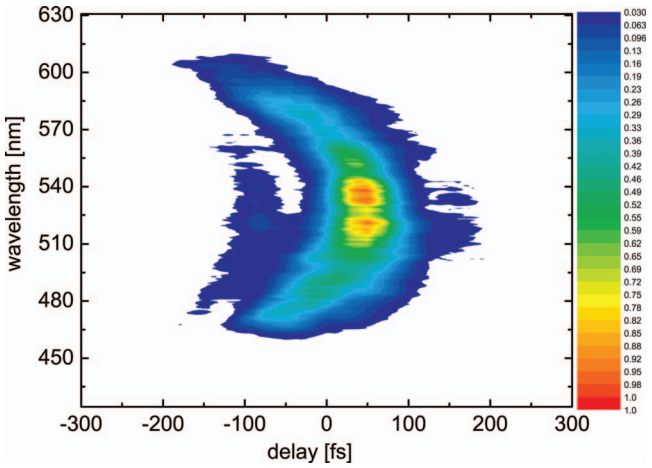

Fig. 4. XFROG trace of the WLC amplified in the 5 mm thick BIBO using probe pulses at 800 nm.

The presented experimental results confirm that BIBO possesses a unique combination of excellent properties for efficient ultrabroadband amplification in the near IR when pumped near 800 nm in a simple collinear geometry. Future efforts will be devoted to the study of slightly noncollinear OPA in BIBO using suitably chirped seed pulses for realization of chirped pulse OPA with subsequent compression, as well as to the study of optical parametric generation of WLC in a single step using again pump pulses near 800 nm.

This work was supported by the German–Bulgarian Exchange Programme (DAAD Grant D/05/11319 and Bulgarian Ministry of Education and Science Grant D01-81/2006).

References

1. M. Raytchev, E. Pandurski, I. Buchvarov, C. Modrakowski, and T. Fiebig, J. Phys. Chem. A **107**, 4592 (2003).
2. Y. Wang, Y. Zhao, J. S. Nelson, Z. Chen, and R. S. Windeler, Opt. Lett. **28**, 182 (2003).
3. A. A. Mikhailovsky, M. A. Petruska, M. I. Stockman, and V. I. Klimov, Opt. Lett. **28**, 1686 (2003).
4. A. Baltuska, T. Fuji, and T. Kobayashi, Opt. Lett. **27**, 306 (2002).
5. A. Brodeur and S. L. Chin, J. Opt. Soc. Am. B **16**, 637 (1999).
6. G. Cerullo and S. De Silvestri, Rev. Sci. Instrum. **74**, 1 (2003).
7. B. Bareika, A. Birmontas, G. Dikchyus, A. Piskarskas, V. Sirutkaitis, and A. Stabinis, Sov. J. Quantum Electron. **12**, 1654 (1982) [Kvantovaya Elektron. (Moscow) **9**, 2534 (1982)].
8. S. N. Orlov, E. V. Pestryakov, and Yu. N. Polivanov, Quantum Electron. **34**, 477 (2004) [Kvantovaya Elektron. (Moscow) **34**, 477 (2004)].
9. M. Tiihonen, V. Pasiskevicius, A. Fragemann, C. Canalias, and F. Laurell, Appl. Phys. B **85**, 73 (2006).
10. N. Umemura, K. Miyata, and K. Kato, Opt. Mater. **30**, 532 (2007).
11. V. Petrov, M. Ghotbi, P. Tzankov, F. Noack I. Nikolov, I. Buchvarov, and M. Ebrahim-Zadeh, Proc. SPIE **6455**, 64550C (2007).